



# Genetic ablation of complement C3 attenuates muscle pathology in *dysferlin*-deficient mice

Renzhi Han,<sup>1,2</sup> Ellie M. Frett,<sup>1</sup> Jennifer R. Levy,<sup>1</sup> Erik P. Rader,<sup>1</sup> John D. Lueck,<sup>1</sup> Dimple Bansal,<sup>1</sup> Steven A. Moore,<sup>3</sup> Rainer Ng,<sup>4</sup> Daniel Beltrán-Valero de Bernabé,<sup>1</sup> John A. Faulkner,<sup>4,5</sup> and Kevin P. Campbell<sup>1</sup>

<sup>1</sup>Howard Hughes Medical Institute, Department of Molecular Physiology and Biophysics, Department of Neurology, Department of Internal Medicine, Roy J. and Lucille A. Carver College of Medicine, The University of Iowa, Iowa City, Iowa, USA. <sup>2</sup>Department of Cell and Molecular Physiology, Loyola University Chicago, Maywood, Illinois, USA. <sup>3</sup>Department of Pathology, Roy J. and Lucille A. Carver College of Medicine, The University of Iowa, Iowa City, Iowa, USA. <sup>4</sup>Department of Molecular and Integrative Physiology and <sup>5</sup>Department of Biomedical Engineering, University of Michigan, Ann Arbor, Michigan, USA.

**Mutations in the *dysferlin* gene underlie a group of autosomal recessive muscle-wasting disorders denoted as dysferlinopathies. Dysferlin has been shown to play roles in muscle membrane repair and muscle regeneration, both of which require vesicle-membrane fusion. However, the mechanism by which muscle becomes dystrophic in these disorders remains poorly understood. Although muscle inflammation is widely recognized in dysferlinopathy and dysferlin is expressed in immune cells, the contribution of the immune system to the pathology of dysferlinopathy remains to be fully explored. Here, we show that the complement system plays an important role in muscle pathology in dysferlinopathy. Dysferlin deficiency led to increased expression of complement factors in muscle, while muscle-specific transgenic expression of dysferlin normalized the expression of complement factors and eliminated the dystrophic phenotype present in *dysferlin*-null mice. Furthermore, genetic disruption of the central component (C3) of the complement system ameliorated muscle pathology in *dysferlin*-deficient mice but had no significant beneficial effect in a genetically distinct model of muscular dystrophy, *mdx* mice. These results demonstrate that complement-mediated muscle injury is central to the pathogenesis of dysferlinopathy and suggest that targeting the complement system might serve as a therapeutic approach for this disease.**

## Introduction

The *dysferlin* gene is located at chromosome 2p13 and contains over 55 exons. The major transcript is 8.5 kb in length and is expressed strongly in striated muscle and the placenta (1, 2). Mutations in the *dysferlin* gene lead to several types of muscle-wasting diseases denoted as dysferlinopathies – limb-girdle muscular dystrophy type 2B (LGMD2B) (1, 2), Miyoshi myopathy (MM) (2), and a distal anterior compartment myopathy (DACM) (3). Dysferlinopathies have also been shown to be associated with a late-onset dilative cardiomyopathy (4–6). Dysferlin is a 230-kDa protein that is widely expressed in different tissues and cells including striated muscle (7) and immune cells (8–10). Previous work using *dysferlin* mutant mice demonstrated that dysferlin plays an essential role in cell membrane repair of striated muscle (5, 11–15). However, it is not fully understood what physiological events lead to muscle pathogenesis when the membrane repair is compromised in dysferlinopathy.

Lengthening contractions (LCs) may cause muscle damage, but several lines of evidence suggest that LCs are not a unique or critical factor for muscle pathogenesis in dysferlinopathy. First, many dysferlinopathy patients were reported to be athletically gifted at a young age and they did not show significant muscle pathology during these sporting activities (16, 17). Second, increased susceptibility to contraction-induced injury of the muscle mem-

brane is usually caused by the loss of the dystrophin-glycoprotein complex (DGC); however, *dysferlin*-deficient skeletal muscle possesses a structurally intact and stable DGC (11). Indeed, recent data showed that *dysferlin*-deficient skeletal muscles are equal to normal skeletal muscles in resistance to contraction-induced injury (18). However, following either 15 repetitive large-strain LCs or 150 small-strain LCs, *dysferlin*-null muscles were observed to experience a strong inflammatory response that delayed their recovery from injury caused by LCs (19, 20). Although the presence of inflammatory infiltrates in muscle is a characteristic of the inflammatory myopathies such as polymyositis and dermatomyositis, several studies have suggested a prominent inflammatory response in the muscle of dysferlinopathy patients (21–23). In about 25% of the cases, the dysferlinopathy patients were initially misdiagnosed as having polymyositis (24, 25). It is enigmatic that dysferlinopathy triggers a prominent inflammatory response, but recent findings have revealed some potential causes. *Dysferlin*-deficient monocytes from SJL/J mice were reported to have increased phagocytic activity (26), and dysferlin deficiency induces an upregulation of inflammasome (27). However, a more recent study (18) did not find a difference in phagocytic activity of *dysferlin*-deficient monocytes using C57BL/10-SJL.Dysf mice, which have a more controlled genetic background. Instead, the authors reported an impaired secretion of chemotactic molecules in *dysferlin*-deficient myocytes, thus reducing neutrophil recruitment at an early stage of regeneration with subsequent incomplete muscle remodeling and ultimate inflammatory responses and develop-

**Conflict of interest:** The authors have declared that no conflict of interest exists.

**Citation for this article:** *J Clin Invest.* 2010;120(12):4366–4374. doi:10.1172/JCI42390.

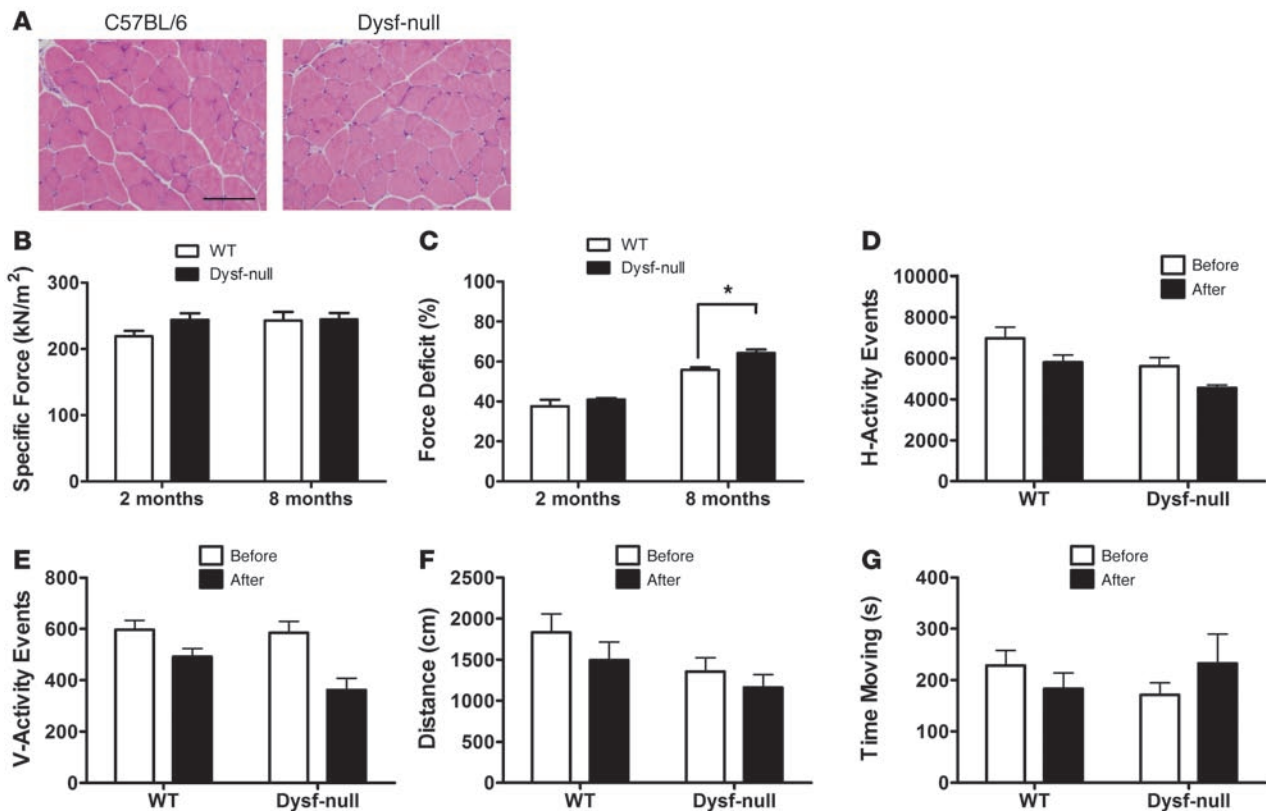


**Figure 1**

Contractile properties of the *dysferlin*-deficient EDL muscles and muscle pathophysiology in response to LCs in vivo. (A) Representative micrographs of H&E-stained EDL muscle sections from C57BL/6 (WT) and *dysferlin*-null (Dysf-null) mice at 8 months of age. Scale bar: 100  $\mu$ m. (B) Muscle-specific force and (C) force deficit after 7 LCs were measured for EDL muscles isolated from WT and *dysferlin*-null mice ( $n = 4$  for each strain at 2 or 8 months of age). Quantified horizontal activity (D), vertical activity (E), travel distance (F), and the moving time (G) before (white columns) and after (black columns) exercise for 2-month-old WT ( $n = 5$ ) and *dysferlin*-null mice ( $n = 4$ ). \* $P < 0.05$ . Data are expressed as mean  $\pm$  SEM.

ment of muscular dystrophy (18). All of these previous findings implicate a complex involvement of the immune system in the pathogenesis of dysferlinopathy.

Our present study identifies the complement system, an important part of the innate immune system that promotes inflammation, as a key player for the pathogenesis of dysferlinopathy. We have shown that the expression of the complement factors are induced in *dysferlin*-deficient skeletal muscle and that genetic ablation of the complement factor C3 ameliorates muscular dystrophy in *dysferlin*-null mice.

## Results

**Contractile properties and muscle pathophysiology in response to LCs.** Muscular dystrophy shows 2 important features: reduced muscle force generation and increased susceptibility to LC-induced damage. We examined the effect of dysferlin deficiency on force production and force deficit in response to LC-induced muscle injury by measuring the in vitro contractile properties of the extensor digitorum longus (EDL) muscles (28) of *dysferlin*-deficient mice and age-matched controls (WT). Unlike quadriceps, the EDL muscle in *dysferlin*-null mice even at 8 months of age had a limited overt pathology (Figure 1A), which allowed us to study the consequence of dysferlin deficiency on contractile properties without preexisting dystrophic alterations. The specific force ( $\text{kN/m}^2$ ) produced

by the *dysferlin*-deficient EDL muscles was not significantly different from that in control muscles at either 2 months ( $219 \pm 8$  in WT vs.  $244 \pm 10$  in *dysferlin*-null;  $n = 4$  for each;  $P = 0.10$ ) or 8 months ( $243 \pm 13$  in WT vs.  $245 \pm 10$  in *dysferlin*-null;  $n = 8$  for each;  $P = 0.92$ ) of age (Figure 1B). These results indicate that dysferlin is not directly involved in the generation of force by skeletal muscles. Previously, Chiu et al. (18) showed that *dysferlin*-deficient tibialis anterior muscle was not susceptible to 1 or 2 LCs with 40% stretch. To detect any subtle difference in the susceptibility to LC-induced damage, we delivered seven 30% stretches to a maximally activated EDL muscles (29), which resulted in a force deficit (percentage of force loss after the stretch protocol) of approximately 37% in WT EDL muscle (Figure 1C). The force deficits in the *dysferlin*-deficient EDL muscle ( $41\% \pm 1\%$  in *dysferlin*-null vs.  $37\% \pm 3\%$  in WT;  $n = 4$  for each;  $P = 0.35$ ) were not significantly different from those in WT EDL muscle at 2 months of age. Even with the stretch level of 40%, the force deficit in the *dysferlin*-deficient EDL muscle at 8 months of age was only slightly increased ( $56\% \pm 1\%$  in WT vs.  $64\% \pm 2\%$  in *dysferlin*-null;  $n = 4$  for each;  $P = 0.01$ ) (Figure 1C).

In order to determine the effect of LC-induced muscle damage in vivo, 2-month-old (prepathological) *dysferlin*-deficient mice were subjected to downhill running. Interestingly, we did not observe a dramatic change in serum creatine kinase (CK) levels (data not shown) or post-run activity (Figure 1, D–G) as compared with

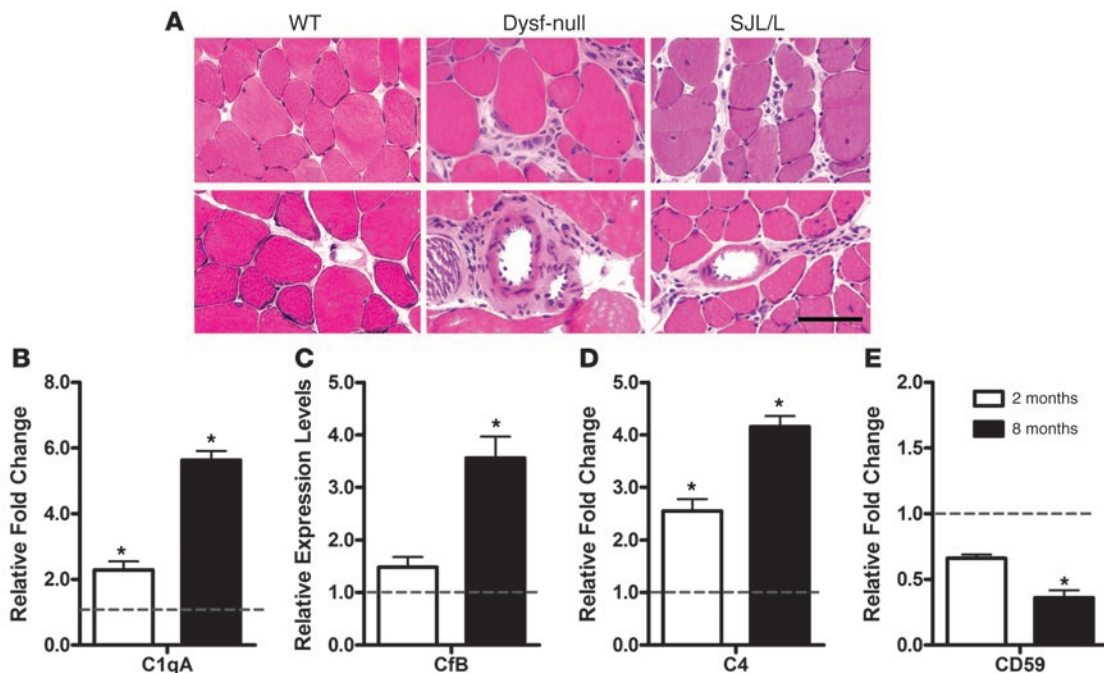


**Figure 2**

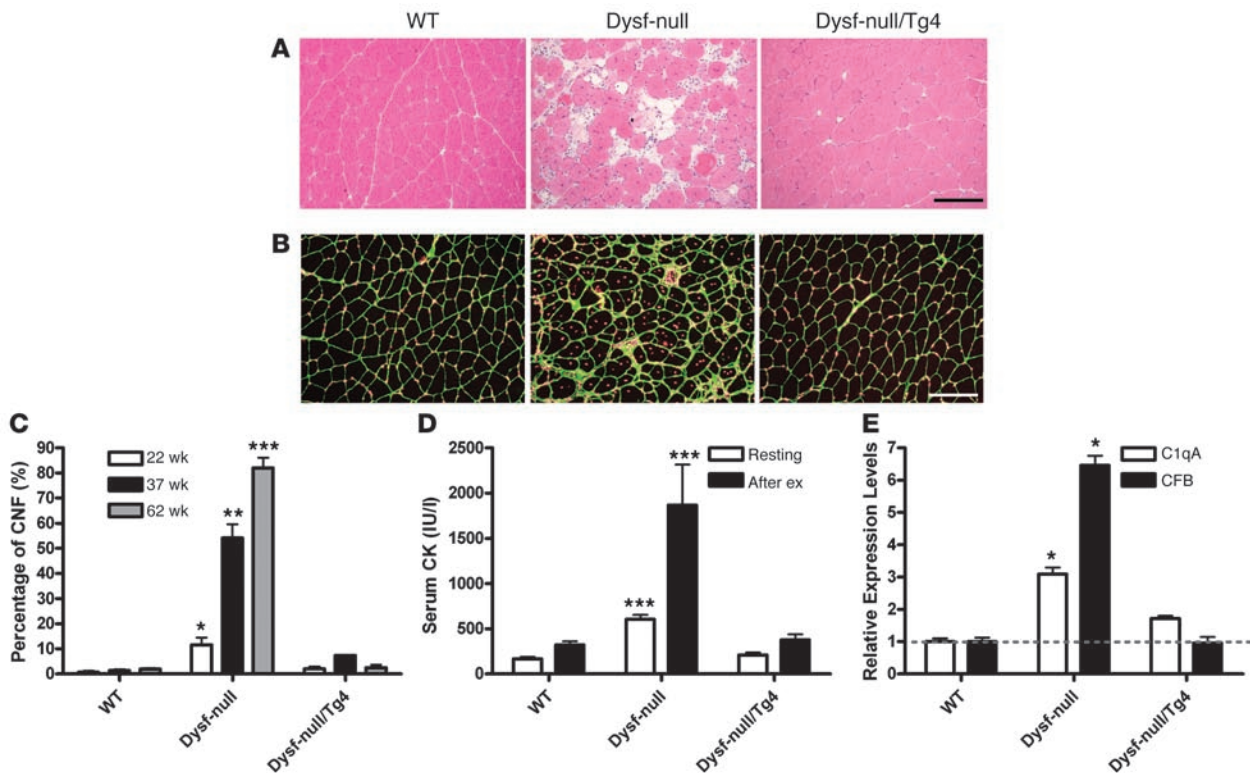
Muscle inflammation and expression of complement factors in *dysferlin*-deficient mice. (A) H&E-stained muscle section of 8-month-old WT, *dysferlin*-null (Dysf-null), and SJL/J mice. Endomysial and perivascular infiltration was observed in both *dysferlin*-null and SJL/J mice. Scale bar: 100  $\mu$ m. (B–E) Real-time quantitative RT-PCR was performed on quadriceps muscles of 2- or 8-month-old *dysferlin*-null versus WT mice ( $n = 3$ ). The mRNA levels of the complement genes were normalized to *Gapdh* mRNA. Expression of C1qA (B), CFB (C), and C4 (D) were elevated during the early and active phases of muscle pathology in *dysferlin*-deficient skeletal muscle compared with levels in skeletal muscle taken from age-matched control mice, whereas the complement inhibitor CD59 (E) was significantly downregulated in old mice. \* $P < 0.05$ . Data are expressed as mean  $\pm$  SEM.

*mdx* mice (30), a mouse model for Duchenne muscular dystrophy (DMD), which carry a mutation in the *dystrophin* gene (31). Importantly, the examiner was blinded to the genotype of the test animals and used a protocol similar to that reported previously (30). These data suggest that *dysferlin*-deficient skeletal muscle is not prone to LC-induced muscle damage as *dystrophin*-deficient skeletal muscle is, and are consistent with the finding that *dysferlin*-deficient skeletal muscle possesses a structurally intact and stable DGC (11). Therefore, in agreement with recent findings (18), our data demonstrate that LC-induced muscle injury alone is not sufficient to cause muscle necrosis in dysferlinopathy.

*Increased proinflammatory gene expression in dysferlin-deficient skeletal muscle.* Similarly to human patients, the *dysferlin*-deficient SJL/J mouse, a natural mouse model of dysferlin deficiency (32), also develops muscular dystrophy with prominent inflammation (33). In addition to developing spontaneous myopathy with inflammation, SJL/J mice are uniquely susceptible to developing experimentally induced myositis (34) and several other autoimmune conditions including experimental autoimmune encephalitis (35). But recently it was shown that the susceptibility to experimental autoimmune encephalomyelitis does not appear to be related to dysferlin deficiency (36). To confirm the correlation of muscle inflammation with dysferlin deficiency, we examined inflammatory features in the skeletal muscle of *dysferlin*-null mice (in C57BL/6 background) through histological and immunofluorescence analyses. Muscle isolated from the mice younger than 4 months of age with little or no muscle pathology did not show inflammatory infiltration (data not

shown). However, muscle isolated from 8-month-old *dysferlin*-null mice had small numbers of infiltrating lymphocytes (Figure 2A). Perivascular as well as endomysial leukocytes were observed in *dysferlin*-null mice. Consistent with previous observations of muscle infiltrate cell populations in *dysferlin*-deficient patients (21–23), approximately 80%–90% of these leukocytes were positive for the macrophage marker Mac-1 (data not shown).

To understand the molecular mechanism of the muscle inflammation in dysferlinopathy, we next sought to identify the proinflammatory genes induced by dysferlin deficiency. We analyzed gene expression profiling data published previously with the use of either *dysferlin*-deficient mouse or human skeletal muscles (14, 37–40). Four of five such microarray studies (14, 37–40) identified the complement factors, including *C1qa*, *C1qb*, *C1qc*, *C4*, *Cfd*, and *DAF*, to be differentially expressed. In order to validate these gene array results, we directly measured the RNA levels of complement factors in skeletal muscle. We performed quantitative real-time RT-PCR on skeletal muscle RNA extracted from 2-month-old (early stage of disease) and 8-month-old (active phase of disease) *dysferlin*-null mice as well as age-matched C57BL/6 controls. The RNA level of the initiating complement factor *C1qa* for the classical complement pathway was elevated in skeletal muscle from the *dysferlin*-deficient mice. The elevation was observed even in the absence of obvious pathology, with levels increased up to 6-fold (when normalized to *GAPDH* RNA) (Figure 2B). Expression of the complement factors *CFB* (alternative pathway-specific component) and *C4* (common component for classical and lectin-mediated

**Figure 3**

Muscle-specific transgenic expression of dysferlin rescues muscle pathology in *dysferlin*-null mice. (A) H&E-stained quadriceps muscle sections of 38-week-old WT, *dysferlin*-null, and *dysferlin*-null/Tg4 mice. The muscle section from *dysferlin*-null showed typical myopathic changes including central nucleation, fiber size variation, inflammation, fibrosis, and fat replacement. No prominent myopathic changes were observed in the *dysferlin*-null/Tg4 muscle. (B) Laminin-stained (green) and DAPI-stained (red) quadriceps muscle section of WT, *dysferlin*-null, and *dysferlin*-null/Tg4 mice. Scale bars: 200  $\mu$ m. (C) Percentage of fibers containing central nuclei (CNF) in the quadriceps muscles of 22-, 37-, and 62-week-old WT, *dysferlin*-null, and *dysferlin*-null/Tg4 mice ( $n = 3$  or 4 for each group; all males). (D) Measurement of serum CK levels in WT, *dysferlin*-null, and *dysferlin*-null/Tg4 mice aged 32–45 weeks before ( $n = 10, 12,$  and  $15,$  respectively) and after ( $n = 4, 3,$  and  $9,$  respectively) downhill running exercise (after ex). (E) Quantitative RT-PCR examination of complement factors C1qA and CFB expression in the quadriceps muscles of WT, *dysferlin*-null and *dysferlin*-null/Tg4 mice ( $n = 3$  for each group). \* $P < 0.05$ ; \*\* $P < 0.01$ ; \*\*\* $P < 0.001$  when compared with the data in either WT or *dysferlin*-null/Tg4. Data are expressed as mean  $\pm$  SEM.

ated pathway) were also elevated in 8-month-old *dysferlin*-deficient skeletal muscle compared with those in age-matched controls (Figure 2, C and D). However, the lectin pathway-specific factor *MASP2* was not significantly affected in *dysferlin*-null muscle from young mice and was slightly downregulated in older mice (Supplemental Figure 1; supplemental material available online with this article; doi:10.1172/JCI42390DS1). In addition, the complement inhibitor CD59 was significantly downregulated in skeletal muscle from old *dysferlin*-null mice (Figure 2E). These data suggest that upregulation of classical and alternative complement pathways and downregulation of complement inhibitors may play a major role in the muscle damage in dysferlinopathy.

*Muscle-specific dysferlin transgenic expression rescues muscle pathology in dysferlin-null mice.* Interestingly, dysferlin has been reported to be expressed in cells of the immune system such as peripheral blood monocytes (8) and neutrophils (41). Although the function of dysferlin in these cells is not clear, dysferlin deficiency was reported recently to increase phagocytic activity in monocytes/macrophages and thus has been proposed as a potential mechanism for the onset of muscle inflammation seen in dysferlinopathy (26). To determine whether the increased phagocytic activity in *dysferlin*-

deficient immune systems is sufficient to cause muscle damage, we generated muscle-specific dysferlin transgenic mice (Supplemental Figure 2). We crossed the *dysferlin*-null mice with a transgenic line (designated as Tg4) in which a single copy of the *dysferlin* transgene is expressed in a skeletal muscle-specific fashion under the control of mouse muscle CK promoter. Dysferlin was overexpressed by approximately 8-fold in these transgenic mice, and they did not show any muscle pathology, while 3 high expression lines showed muscle atrophy (Supplemental Figure 2). The *dysferlin*-null mice at 8 months presented typical myopathic changes, such as central nuclei, fat replacement, necrosis, and regeneration (Figure 3A). These myopathic changes were abrogated in the *dysferlin*-null/Tg4 mice of the same age except that a low percentage of central nuclei were still present (Figure 3A). The centrally nucleated fibers were counted after staining the muscle section with laminin and DAPI (Figure 3B). At 5 months of age, the quadriceps of male *dysferlin*-null mice had  $11.5 \pm 5.8\%$  centrally nucleated fibers, while the quadriceps of the control and *dysferlin*-null/Tg4 mice had only  $0.6 \pm 1.1\%$  and  $2.0 \pm 1.6\%$  (Figure 3C). However, at 8 months of age, the percentage of the central nucleated fibers in the quadriceps of male *dysferlin*-null mice was dramatically increased to  $72.7 \pm 11.4\%$ ,

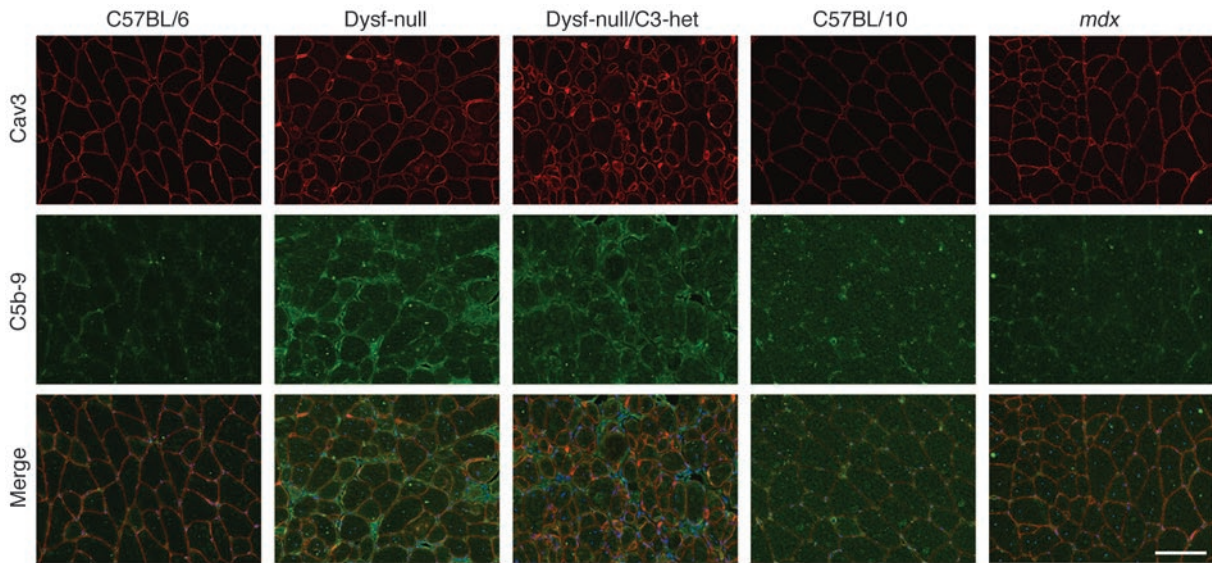


**Figure 4**

Immunofluorescence analysis of complement C5b-9 deposition in mouse skeletal muscles. Immunofluorescence analysis did not detect complement C5b-9 expression in the muscle sections from WT mice (C57BL/6 and C57BL/10) and *mdx* mice but showed that complement C5b-9 was deposited onto the muscle cell membrane in *dysferlin*-null mice. All samples were prepared and processed equally at the same time, and all images were taken at the same exposure level. Scale bar: 100  $\mu$ m.

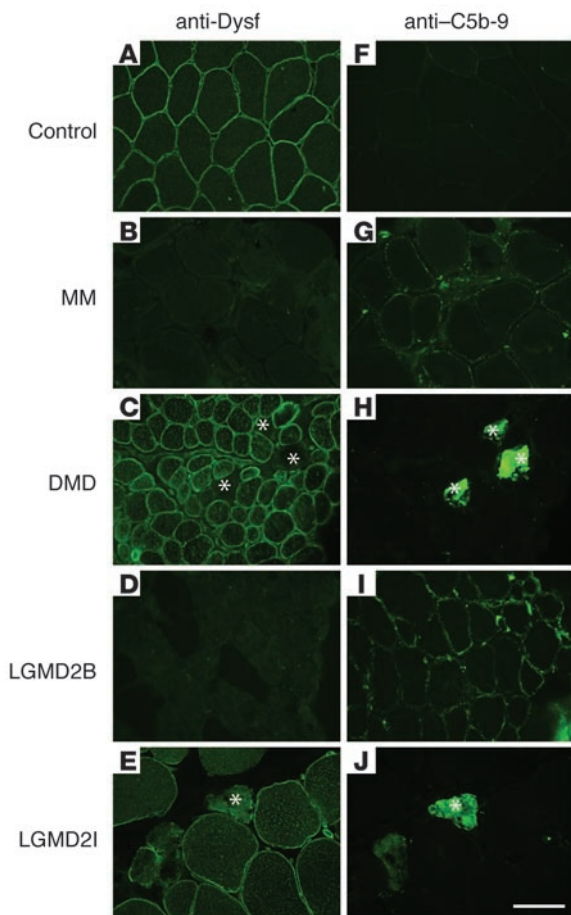
and this number was only slightly increased to  $9.3\% \pm 3.9\%$  in *dysferlin*-null/Tg4 mice (Figure 3C). Serum CK levels of the *dysferlin*-null/Tg4 mice were normal before or after exercise, but those of the *dysferlin*-null were elevated as reported before (Figure 3D). Consistent with a recent report (42), these data suggest that the presence of dysferlin in skeletal muscle protects muscle from damage even in the presence of a *dysferlin*-deficient immune system. Furthermore, quantitative RT-PCR examination of the quadriceps muscles from the *dysferlin*-null/Tg4 mice suggests that transgenic expression of dysferlin normalized the expression of the complement factors *C1qA* and *CFB* (Figure 3E). Taken together, the loss of dysferlin in skeletal muscle induces complement upregulation that may lead to the development of muscle pathology accompanied by inflammation.

**Complement deposits in *dysferlin*-deficient skeletal muscle.** To further determine whether increased complement expression induces complement deposition in *dysferlin*-deficient skeletal muscle, we stained muscle sections of mice with the antibody against C5b-9 to detect dysferlin expression and the formation of the terminal complement activation product – membrane attack complex (MAC). In skeletal muscles of WT mice, no surface deposition of MAC was detected (Figure 4). However, deposition of MAC at the surface of muscle fibers could be discerned in *dysferlin*-null mice (Figure 4). To determine whether the MAC deposition observed in *dysferlin*-null muscle is the consequence of muscular dystrophy, we looked at skeletal muscle from the *mdx* mouse, a mouse model for DMD (31). We did not detect surface MAC staining in skeletal muscle fibers of *mdx* mice, although these mice developed more severe muscular dystrophy than *dysferlin*-null mice (Figure 4).

To test the possibility that the complement deposition shown in *dysferlin*-null skeletal muscle is species specific, we also examined muscle sections from human patients for complement deposition. *Dysferlin*-deficient patient muscle sections were stained with an antibody against dysferlin and an antibody against C5b-9, respectively

(Figure 5, A–J). Dysferlin was not detected in the muscles from MM (Figure 5B) and LGMD2B patients (Figure 5D). As reported previously, increased cytoplasmic dysferlin expression was observed in the muscles from DMD and LGMD2I patients (Figure 5, C and E), as compared with control muscle (Figure 5A). Interestingly, MAC was observed to be widely deposited onto the sarcolemma of skeletal muscle fibers from MM (Figure 5G) and LGMD2B (Figure 5I) patients while not observed in control muscle (Figure 5F). Although positive MAC staining was also observed in DMD muscle sections, it was only observed in necrotic myofibers where it stained the entire cell (Figure 5H). The nonnecrotic fibers are spared for MAC deposition in DMD (Figure 5H). Similar staining for MAC is observed in nondysferlin forms of LGMD such as LGMD2I (Figure 5J). These data suggest that the surface complement deposition is specific for *dysferlin*-deficient skeletal muscle and does not appear to be merely a secondary effect after muscle damage.

**Genetic ablation of C3 ameliorates muscle pathology in *dysferlin*-null mice.** If the complement activation contributes to the muscle damage in dysferlinopathy, we hypothesized that disruption of the complement pathway may ameliorate the dystrophic phenotype in *dysferlin*-null mice. To test this hypothesis, we examined the effect of genetic deletion of the central component (C3) of the complement system on muscle pathology in *dysferlin*-null mice. *Dysferlin*/C3 double-mutant mice were generated by crossing *dysferlin*-null mice with C3-deficient mice, which were made in the laboratory of Michael C. Carroll (43). Both *dysferlin*-null mice and C3-null mice had been backcrossed with C57BL/6 mice for more than 6 generations before they were bred together to generate the double-mutant mice. Disruption of both dysferlin and C3 in *dysferlin*/C3 double-mutant mice was confirmed by Western blotting analysis with the antibodies against dysferlin and C3 (Figure 6A). C3 immunofluorescence analysis of quadriceps muscles showed C3 is widely deposited onto the sarcolemma of *dysferlin*-deficient muscle, while this staining pattern was not observed in either WT or *dysferlin*/C3 double-

**Figure 5**

Immunofluorescence analysis of complement C5b-9 deposition in human patient skeletal muscles. Muscle sections from control (A and F), MM (B and G), DMD (C and H), LGMD2B (D and I), and LGMD2I (E and J) patients were stained with antibodies against dysferlin (A–E) or C5b-9 (F–J). Complement C5b-9 was not present in control patient muscle fibers, but deposited onto the sarcolemma of MM and LGMD2B muscles. In DMD and LGMD2I muscle sections, complement C5b-9 was detected only in the necrotic muscle fibers (H and J). All samples were prepared and processed equally at the same time, and all images were taken at the same exposure level. Scale bar: 100  $\mu$ m. Asterisks indicate necrotic muscle fibers.

the double-mutant mice (Figure 7D). Compared with the muscles from *dysferlin*-null mice, the muscles from *dysferlin/C3* double-mutant mice showed a more uniform profile of myofiber areas, fewer smaller fibers, and a greater number of larger fibers than in WT mice (Figure 7E). To determine whether the effect of C3 ablation is common across other dystrophic models, we also crossed the C3-null mice with *mdx* mice to generate dystrophin/C3 double-mutant mice (*mdx/C3*-null) and studied the muscle pathology of the breeding progeny. Disruption of dystrophin and C3 expression in the *mdx/C3*-null mice was confirmed by Western blotting analysis of total muscle extracts (Supplemental Figure 3). Quadriceps muscle pathology among the progeny was similarly analyzed, as mentioned above. No significant improvements in muscle pathology were detected in *mdx/C3*-null mice when compared with *mdx* mice (Supplemental Figure 4).

The pathological effects of complement activation are mediated directly by MAC and indirectly by C3a and C5a factors that stimulate a range of proinflammatory responses from mast cells and leukocytes. To further determine whether MAC formation is the cause of muscle damage in dysferlinopathy, we generated *dysferlin/C5* double-mutant mice. Histological examination of quadriceps muscle from the double-mutant mice did not reveal remarkable improvement in dystrophic features (Supplemental Figure 5). Quantitative analysis showed the same size distribution pattern and similar percentage of central nucleated myofibers in *dysferlin/C5* double-mutant mice as in *dysferlin* single-mutant mice (Supplemental Figure 5). These data suggest that the terminal activation of complement has minimal effect on disease progression in dysferlinopathy.

## Discussion

Collectively, our data show that loss of dysferlin in skeletal muscle induces the expression of complement factors, with the largest expression changes observed in the initiating factors C1q in the classical pathway and the alternative pathway factor CFB. Furthermore, disruption of the complement system mitigates muscle pathology in *dysferlin*-deficient mice. The complement system not only plays an important role in the immune defense system, but also contributes to the amplification of inflammation, if activated in excess, or is inappropriately controlled. Activation of the complement system causes tissue injury in animal models of autoimmune diseases, such as glomerulonephritis, hemolytic anemia, myasthenia gravis, and in 2 nonimmunologically mediated forms of primary tissue damage, burn, and ischemia (reviewed in ref. 45). In the present study, we showed that complement activation contributes to muscle injury in dysferlinopathy. Disruption of the central component (C3) of the complement system attenuates the pathological alterations in *dysferlin*-deficient skeletal muscle, but

null mice (Figure 6B). To determine whether C3 ablation affects the membrane repair capacity of muscle fibers, we performed the laser-induced membrane damage and repair assay (5, 11, 44) on the muscle fibers isolated from either WT, *dysferlin*-null, C3-null, or *dysferlin/C3* double-null mice. As expected, we found that C3 ablation did not have any significant effect on the membrane-repair capacity of muscle fibers (Figure 6C).

Since contractile dysfunction could hardly be discerned in EDL muscles of *dysferlin*-null mice even at 8 months of age (Figure 1B), we did not examine the effect of C3 ablation on the force development of EDL muscles. To assess the effect of C3 ablation on muscle pathology in *dysferlin*-null mice, we compared the quadriceps muscle pathology among the mice with different genotypes using histological analysis. By 5 months, the quadriceps muscles from female *dysferlin*-null mice developed an overt dystrophic phenotype including central nucleation, fiber size variation, hypertrophic myofibers, fibrosis, and fat replacement (Figure 7A). Deletion of the C3 gene decelerated this process significantly and maintained relatively normal muscle histology (Figure 7C). Disruption of only 1 copy of the C3 gene was not sufficient to alleviate the dystrophic features in *dysferlin*-null mice (Figure 7B). To more carefully analyze the phenotype of *dysferlin/C3* double-mutant mice, we quantified the myofiber areas and the percentage of central nucleation of myofibers. Quadriceps muscle from *dysferlin*-null mice showed the characteristic increase in central nucleation of myofibers owing to ongoing degeneration and regeneration, and this degeneration/regeneration cycle was significantly reduced in

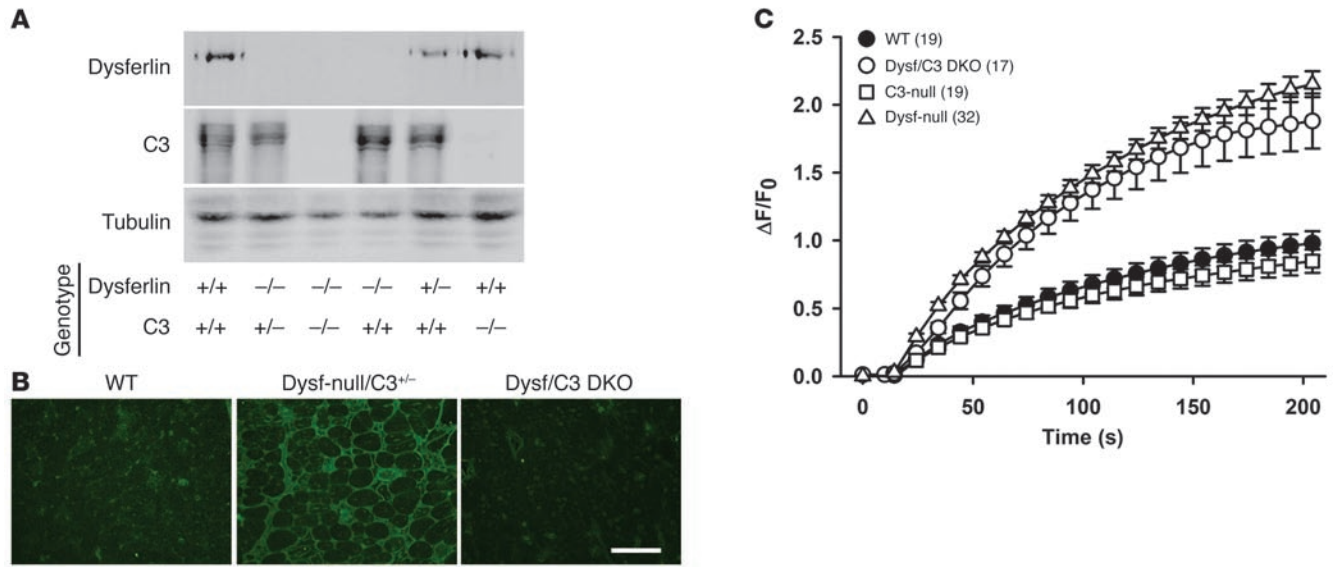


**Figure 6** Generation and characterization of *dysferlin/C3* double-mutant (*Dystf/C3* DKO) mice. **(A)** Western blotting analysis of skeletal muscle microsomes prepared from the mice of different genotypes as designated. The expression of dysferlin and C3 was disrupted in the *dysferlin/C3* double-null mice. **(B)** C3 immunofluorescence staining of quadriceps muscle sections from WT, *dysferlin*-null/*C3*<sup>+/-</sup>, and *dysferlin/C3* double-null mice. Scale bar: 200 μm. **(C)** Quantitative analysis of FM 1-43 fluorescence intensity changes ( $\Delta F/F_0$ ) following laser-induced membrane damage showed that the membrane repair capacity of muscle fibers was compromised in *dysferlin*-null mice (triangles) compared with WT (black circles), but disruption of C3 did not significantly affect the membrane repair efficiency in either WT (squares) or *dysferlin*-null background (white circles). The numbers in parentheses are the numbers of fibers examined. Data are expressed as mean  $\pm$  SEM.

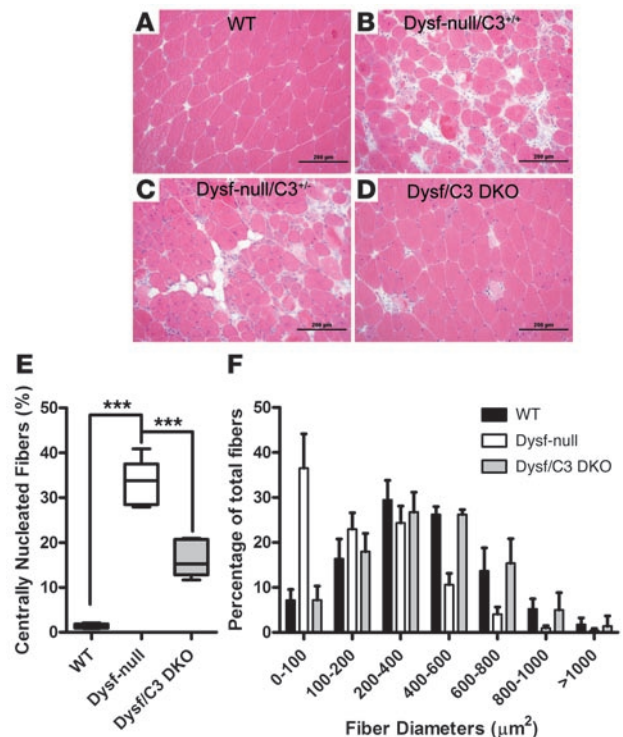
genetic ablation of the terminal component (C5) of the complement system has minimal effect on muscle pathology in *dysferlin*-deficient mice. These results suggest that it is not the terminal activation of the complement system but the activation of C3 that accelerates muscle injury in *dysferlin*-null mice.

Dysferlin has been shown to play roles in various cellular activities of muscle including membrane repair (5, 11–15), muscle differentiation (46), muscle regeneration, and cytokine release (18), all of which may rely on the function of dysferlin in promoting membrane fusion. It is still not clear why dysferlinopathy shows such a broad clinical spectrum and such extensive muscle inflammation. The age of onset of dysferlinopathy varies widely, from 12 to 59 years (47). Recently, an unusual case was reported in which a patient with complete loss of dysferlin showed the first symptoms at the age of 73 years and remained fully ambulant even at 85 years old (48). These observations are in contrast to a mean age of 34 years at the first use of wheelchair and nearly 30% of dysferlinopathy patients being wheelchair dependent after 15 years of disease diagnosis (25). Our study identified the complement

immune system as an important factor affecting the progression of muscle pathology in dysferlinopathy. This finding also provides important insights into the design of novel therapeutic strategies for these patients.

**Figure 7**

Amelioration of muscle pathology in *dysferlin*-deficient mice by genetic ablation of complement factor C3. **(A–D)** Representative H&E-stained histology of quadriceps muscles from WT **(A)**, *dysferlin*-null/*C3*<sup>+/-</sup> **(B)**, *dysferlin*-null/*C3*<sup>+/-</sup> **(C)**, and *dysferlin/C3* double-null littermates **(D)** at 23 weeks of age. Scale bars: 200 μm. **(E)** Percentage of fibers containing central nuclei in the quadriceps muscles of 23-week-old WT, *dysferlin*-null, and *dysferlin/C3* double-null mice (*n* = 5 for each group). **(F)** Fiber areas (grouped into size ranges) from quadriceps muscles of 23-week-old WT, *dysferlin*-null, and *dysferlin/C3* double-null mice (*n* = 5 for each group). \*\*\**P* < 0.01. Data are expressed as mean  $\pm$  SEM.





It is not known how complement is activated in dysferlinopathy. At least 3 potential mechanisms are involved (Supplemental Figure 6). First, damaged cells release a number of constitutively expressed proteins, such as heat shock proteins (49), the chromatin HMGB1, and mitochondrial peptides bearing the N-formal group that are characteristic of prokaryotic proteins (50), all of which have been shown to activate the complement system. The heat shock proteins can activate the complement system in both an antibody-dependent and -independent manner, and this occurs in the absence of pathogens (51). HMGB1, which is secreted by activated monocytes and macrophages and passively released by necrotic or damaged cells, also potentially induces complement activation and inflammation (50). Therefore, even aseptic tissue injury activates the complement cascade. The loss of dysferlin-mediated membrane repair would be expected to lead to a continuous leakage of cytosolic contents following any incurred membrane damage, and this in turn would result in continuous complement activation. In this scenario, the complement pathway would function as an amplifier of muscle membrane damage that occurs due to the absence of dysferlin. Second, failure of the release of cytokines from damaged muscle in dysferlinopathy (18) may account for the impairment of inflammatory cell recruitment at an early stage of muscle regeneration, with subsequent incomplete muscle remodeling, resulting in abnormal activation of the complement system. Finally, both dysferlin (11, 14) and synaptotagmin VII (52, 53) have been reported to play a role in membrane repair. Synaptotagmin VII primarily mediates the fusion of lysosomes with plasma membrane (45), while the vesicle compartments utilized by dysferlin-mediated membrane repair have not as yet been identified. It is likely that both dysferlin-mediated membrane repair and synaptotagmin VII-mediated membrane repair play roles in normal skeletal muscle maintenance, as genetic disruption of either dysferlin or synaptotagmin VII leads to the development of myopathies in mice (11, 52). In the absence of dysferlin, skeletal muscle may thus primarily utilize the synaptotagmin VII-mediated membrane repair pathway with lysosomes to reseal membrane damage. A recent study (54) showed that persistent fusion of lysosomes with plasma membrane during the suicidal membrane repair prior to apoptosis causes the externalization of phosphatidylserine (PS) on the outer leaflet of the cell membrane. The PS exposure induces inflammatory responses that preclude the development of tumor- and patient-specific immune responses during chemotherapy and radiotherapy. Interestingly, C1q, the recognition unit of the C1 complex of complement, was shown to bind PS and likely acts as a multi-ligand-bridging molecule in apoptotic cell recognition (55). Therefore, it is likely that persistent utilization of lysosomes for membrane repair in *dysferlin*-deficient skeletal muscle induces PS externalization that activates complement pathways through binding C1q and triggers muscle damage.

## Methods

For details of mice, antibodies, reagents, and analysis, see Supplemental Methods.

**Mouse models.** Mice (*dysferlin*-null, SJL/J, *mdx*, *dysferlin*/C3-null, *dysferlin*/C5-null, *mdx*/C3-null, and WT littermate control mice) were maintained at The University of Iowa Animal Care Unit in accordance with animal use guidelines. All animal studies were authorized by the Animal Care, Use, and Review Committee of The University of Iowa.

**Measurement of contractile properties.** Muscle mass, fiber length, and maximum force were measured on 8 EDL muscles from 2- and 8-month-old

WT and *dysferlin*-null mice ( $n = 4$  for each group). Total cross-sectional area (CSA,  $\text{cm}^2$ ) and specific force  $P_0$  ( $\text{kN}/\text{m}^2$ ) were determined (28, 44). The susceptibility of muscles to contraction-induced injury was assessed by 7 LCs with a strain of 30% of fiber length (30, 49). The differences between the experimental and WT samples were assessed by a 2-tailed Student's *t* test, with the assumption of 2-sample equal variance.

**Treadmill exercise and activity monitoring.** Animals were mildly exercised using an adjustable variable speed belt treadmill from AccuPacer. Activity based on ambulatory behavior was assessed in an open-field test as described in Supplemental Methods.

**H&E staining and immunofluorescence analysis.** Seven-micron muscle cryosections were prepared from quadriceps and iliopsoas muscles of the aforementioned mice. Routine H&E staining and immunofluorescence staining were used to examine the muscle histopathology. The areas of muscle fibers and the percentage of central nucleated muscle fibers were calculated using Image-Pro Plus 6.

**Statistics.** Unless otherwise stated, the data were calculated according to an analysis of variance and expressed as mean  $\pm$  SEM. Where appropriate, the significance of differences between multiple genetically defined mouse models and their WT counterparts was assessed using 1-way ANOVA with Bonferroni's post-tests, and the significance of differences between 2 experimental groups was assessed by unpaired 2-tailed Student's *t* test.  $P < 0.05$  was accepted as significant.

## Acknowledgments

We thank Keith Garringer, Sally Prouty, Taylor Peterson, and Robert Crawford for technical support and all members of the Campbell laboratory for fruitful discussions. This work was supported in part by an American Heart Association Scientist Development grant (10SDG4140138 to R. Han), a Muscular Dystrophy Association Research grant (MDA171667 to R. Han), a Paul D. Wellstone Muscular Dystrophy Cooperative Research Center grant (1U54NS053672 to K.P. Campbell), a Muscular Dystrophy Association grant (MDA3936, to K.P. Campbell), and a U.S. Department of Defense grant (W81XWH-05-1-0079). We also thank the University of Iowa Roy J. and Lucille A. Carver College of Medicine, the Senator Paul D. Wellstone Muscular Dystrophy Cooperative Research Center, and the University of Iowa Central Microscopy Research Facility. Transgenic mice were generated at the University of Iowa Transgenic Animal Facility directed by Curt D. Sigmund, and this facility was supported in part by grants from the NIH and from the Roy J. and Lucille A. Carver College of Medicine. We wish to thank Norma Sinclair, Patricia Yarolem, and Joanne Schwartz for their technical expertise in generating transgenic mice. K.P. Campbell is an investigator of the Howard Hughes Medical Institute. J.D. Lueck is supported by a Myotonic Dystrophy Foundation postdoctoral fellowship (MDF-FF-2009-0002). J.R. Levy is supported by NIH grant T32HL007121 through NHLBI. E.P. Rader is supported by a Muscular Dystrophy Association development grant (award ID 67814).

Received for publication January 20, 2010, and accepted in revised form September 15, 2010.

Address correspondence to: Kevin P. Campbell, Howard Hughes Medical Institute, Department of Molecular Physiology and Biophysics, The University of Iowa Carver College of Medicine, 4283 CBRB, 285 Newton Road, Iowa City, Iowa 52242-1101, USA. Phone: 319.335.7867; Fax: 319.335.6957; E-mail: kevin-campbell@uiowa.edu.



1. Bashir R, et al. A gene related to Caenorhabditis elegans spermatogenesis factor fer-1 is mutated in limb-girdle muscular dystrophy type 2B. *Nat Genet.* 1998; 20(1):37–42.
2. Liu J, et al. Dysferlin, a novel skeletal muscle gene, is mutated in Miyoshi myopathy and limb girdle muscular dystrophy. *Nat Genet.* 1998;20(1):31–36.
3. Illa I, et al. Distal anterior compartment myopathy: a dysferlin mutation causing a new muscular dystrophy phenotype. *Ann Neurol.* 2001;49(1):130–134.
4. Kuru S, et al. A patient with limb girdle muscular dystrophy type 2B (LGMD2B) manifesting cardiomyopathy [in Japanese]. *Rinsho Shinkeigaku.* 2004;44(6):375–378.
5. Han R, et al. Dysferlin-mediated membrane repair protects the heart from stress-induced left ventricular injury. *J Clin Invest.* 2007;117(7):1805–1813.
6. Chase TH, Cox GA, Burzenski L, Foreman O, Shultz LD. Dysferlin deficiency and the development of cardiomyopathy in a mouse model of limb-girdle muscular dystrophy 2B. *Am J Pathol.* 2009;175(6):2299–2308.
7. Anderson LV, et al. Dysferlin is a plasma membrane protein and is expressed early in human development. *Hum Mol Genet.* 1999;8(5):855–861.
8. Ho M, Gallardo E, McKenna-Yasek D, De Luna N, Illa I, Brown RH Jr. A novel, blood-based diagnostic assay for limb girdle muscular dystrophy 2B and Miyoshi myopathy. *Ann Neurol.* 2002;51(1):129–133.
9. Jethwaney D, et al. Proteomic analysis of plasma membrane and secretory vesicles from human neutrophils. *Proteome Sci.* 2007;5:12.
10. De Luna N, et al. Dysferlin expression in monocytes: a source of mRNA for mutation analysis. *Neuromuscul Disord.* 2007;17(1):69–76.
11. Bansal D, et al. Defective membrane repair in dysferlin-deficient muscular dystrophy. *Nature.* 2003; 423(6936):168–172.
12. Cenacchi G, Fanin M, De Giorgi LB, Angelini C. Ultrastructural changes in dysferlinopathy support defective membrane repair mechanism. *J Clin Pathol.* 2005;58(2):190–195.
13. Cai C, et al. Membrane repair defects in muscular dystrophy are linked to altered interaction between MG53, caveolin-3, and dysferlin. *J Biol Chem.* 2009; 284(23):15894–15902.
14. Lennon NJ, Kho A, Bacskai BJ, Perlmutter SL, Hyman BT, Brown RH Jr. Dysferlin interacts with annexins A1 and A2 and mediates sarcolemmal wound-healing. *J Biol Chem.* 2003;278(50):50466–50473.
15. Hino M, et al. Insufficient membrane fusion in dysferlin-deficient muscle fibers after heavy-ion irradiation. *Cell Struct Funct.* 2009;34(1):11–15.
16. Klinge L, et al. New aspects on patients affected by dysferlin deficient muscular dystrophy. *J Neurol Neurosurg Psychiatry.* 2010;81(9):946–953.
17. Mahjneh I, Marconi G, Bushby K, Anderson LV, Tolvanen-Mahjneh H, Somer H. Dysferlinopathy (LGMD2B): a 23-year follow-up study of 10 patients homozygous for the same frameshifting dysferlin mutations. *Neuromuscul Disord.* 2001;11(1):20–26.
18. Chiu YH, et al. Attenuated muscle regeneration is a key factor in dysferlin-deficient muscular dystrophy. *Hum Mol Genet.* 2009;18(11):1976–1989.
19. Roche JA, Lovering RM, Roche R, Ru LW, Reed PW, Bloch RJ. Extensive mononuclear infiltration and myogenesis characterize the recovery of dysferlin-null skeletal muscle from contraction-induced injuries. *Am J Physiol Cell Physiol.* 2010;298(2):C298–C312.
20. Roche JA, Lovering RM, Bloch RJ. Impaired recovery of dysferlin-null skeletal muscle after contraction-induced injury in vivo. *Neuroreport.* 2008; 19(16):1579–1584.
21. Gallardo E, Rojas-Garcia R, de Luna N, Pou A, Brown RH Jr, Illa I. Inflammation in dysferlin myopathy: immunohistochemical characterization of 13 patients. *Neurology.* 2001;57(11):2136–2138.
22. Fanin M, Angelini C. Muscle pathology in dysferlin deficiency. *Neuropathol Appl Neurobiol.* 2002;28(6):461–470.
23. Confalonieri P, et al. Muscle inflammation and MHC class I up-regulation in muscular dystrophy with lack of dysferlin: an immunopathological study. *J Neuroimmunol.* 2003;142(1–2):130–136.
24. Selva-O'Callaghan A, Labrador-Horrillo M, Gallardo E, Herruzo A, Grau-Junyent JM, Vilardell-Tarres M. Muscle inflammation, autoimmune Addison's disease and sarcoidosis in a patient with dysferlin deficiency. *Neuromuscul Disord.* 2006;16(3):208–209.
25. Nguyen K, et al. Phenotypic study in 40 patients with dysferlin gene mutations: high frequency of atypical phenotypes. *Arch Neurol.* 2007;64(8):1176–1182.
26. Nagaraju K, et al. Dysferlin deficiency enhances monocyte phagocytosis: a model for the inflammatory onset of limb-girdle muscular dystrophy 2B. *Am J Pathol.* 2008;172(3):774–785.
27. Rawat R, Cohen TV, Ampong B, Francia D, Henriques-Pons A, Hoffman EP, Nagaraju K. Inflammation up-regulation and activation in dysferlin-deficient skeletal muscle. *Am J Pathol.* 2010;176(6):2891–2900.
28. Brooks SV, Faulkner JA. Contractile properties of skeletal muscles from young, adult and aged mice. *J Physiol.* 1988;404:71–82.
29. DelloRusso C, Crawford RW, Chamberlain JS, Brooks SV. Tibialis anterior muscles in mdx mice are highly susceptible to contraction-induced injury. *J Muscle Res Cell Motil.* 2001;22(5):467–475.
30. Kobayashi YM, et al. Sarcolemma-localized nNOS is required to maintain activity after mild exercise. *Nature.* 2008;456(7221):511–515.
31. Sicinski P, Geng Y, Ryder-Cook AS, Barnard EA, Darlison MG, Barnard PJ. The molecular basis of muscular dystrophy in the mdx mouse: a point mutation. *Science.* 1989;244(4912):1578–1580.
32. Bittner RE, et al. Dysferlin deletion in SJL mice (SJL-Dysf) defines a natural model for limb girdle muscular dystrophy 2B. *Nat Genet.* 1999;23(2):141–142.
33. Nemoto H, Konno S, Nakazora H, Miura H, Kurihara T. Histological and immunohistological changes of the skeletal muscles in older SJL/J mice. *Eur Neurol.* 2007;57(1):19–25.
34. Rosenberg NL, Ringel SP, Kotzin BL. Experimental autoimmune myositis in SJL/J mice. *Clin Exp Immunol.* 1987;68(1):117–129.
35. Bernard CC, Carnegie PR. Experimental autoimmune encephalomyelitis in mice: immunologic response to mouse spinal cord and myelin basic proteins. *J Immunol.* 1975;114(5):1537–1540.
36. Hochmeister S, Bittner RE, Hoyer H, Lassmann H, Bradl M. The susceptibility to experimental autoimmune encephalomyelitis is not related to dysferlin-deficiency. *Autoimmunity.* 2009;42(3):235–241.
37. Campanaro S, et al. Gene expression profiling in dysferlinopathies using a dedicated muscle microarray. *Hum Mol Genet.* 2002;11(26):3283–3298.
38. Suzuki N, et al. Expression profiling with progression of dystrophic change in dysferlin-deficient mice (SJL). *Neurosci Res.* 2005;52(1):47–60.
39. von der Hagen M, et al. The differential gene expression profiles of proximal and distal muscle groups are altered in pre-pathological dysferlin-deficient mice. *Neuromuscul Disord.* 2005;15(12):863–877.
40. Wenzel K, et al. Increased susceptibility to complement attack due to down-regulation of decay-accelerating factor/CD55 in dysferlin-deficient muscular dystrophy. *J Immunol.* 2005;175(9):6219–6225.
41. Feuk-Lagerstedt E, Movitz C, Pellme S, Dahlgren C, Karlsson A. Lipid raft proteome of the human neutrophil azurophil granule. *Proteomics.* 2007; 7(2):194–205.
42. Millay DP, et al. Genetic manipulation of dysferlin expression in skeletal muscle: novel insights into muscular dystrophy. *Am J Pathol.* 2009;175(5):1817–1823.
43. Wessels MR, Butko P, Ma M, Warren HB, Lage AL, Carroll MC. Studies of group B streptococcal infection in mice deficient in complement component C3 or C4 demonstrate an essential role for complement in both innate and acquired immunity. *Proc Natl Acad Sci U S A.* 1995;92(25):11490–11494.
44. Han R, et al. Basal lamina strengthens cell membrane integrity via the laminin G domain-binding motif of alpha-dystroglycan. *Proc Natl Acad Sci U S A.* 2009;106(31):12573–12579.
45. Morgan BP. Complement membrane attack on nucleated cells: resistance, recovery and non-lethal effects. *Biochem J.* 1989;264(1):1–14.
46. de Luna N, et al. Absence of dysferlin alters myogenin expression and delays human muscle differentiation “in vitro”. *J Biol Chem.* 2006;281(25):17092–17098.
47. Ueyama H, Kumamoto T, Horinouchi H, Fujimoto S, Aono H, Tsuda T. Clinical heterogeneity in dysferlinopathy. *Intern Med.* 2002;41(7):532–536.
48. Klinge L, et al. Late onset in dysferlinopathy widens the clinical spectrum. *Neuromuscul Disord.* 2008; 18(4):288–290.
49. Basu S, Binder RJ, Suto R, Anderson KM, Srivastava PK. Necrotic but not apoptotic cell death releases heat shock proteins, which deliver a partial maturation signal to dendritic cells and activate the NF-kappa B pathway. *Int Immunol.* 2000;12(11):1539–1546.
50. Scaffidi P, Misteli T, Bianchi ME. Release of chromatin protein HMGB1 by necrotic cells triggers inflammation. *Nature.* 2002;418(6894):191–195.
51. Prohaszka Z, et al. Heat shock protein 70 is a potent activator of the human complement system. *Cell Stress Chaperones.* 2002;7(1):17–22.
52. Chakrabarti S, et al. Impaired membrane resealing and autoimmune myositis in synaptotagmin VII-deficient mice. *J Cell Biol.* 2003;162(4):543–549.
53. Reddy A, Caler EV, Andrews NW. Plasma membrane repair is mediated by Ca(2+)-regulated exocytosis of lysosomes. *Cell.* 2001;106(2):157–169.
54. Mirnikjoo B, Balasubramanian K, Schroit AJ. Suicidal Membrane Repair Regulates Phosphatidylserine Externalization during Apoptosis. *J Biol Chem.* 2009;284(34):22512–22516.
55. Paidassi H, et al. C1q binds phosphatidylserine and likely acts as a multiligand-bridging molecule in apoptotic cell recognition. *J Immunol.* 2008; 180(4):2329–2338.

## Supplemental Figures

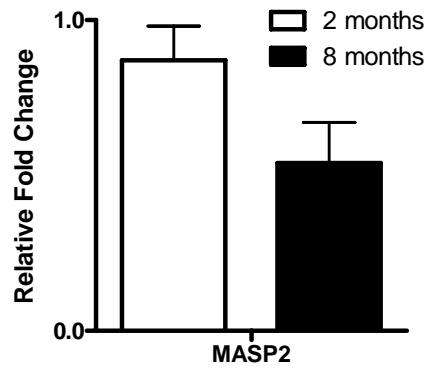


**Figure S1. Expression of *MASP2* in dysferlin-deficient skeletal muscle.** Real-time quantitative RT-PCR was performed on quadriceps muscles of 2- or 8-month-old dysferlin-null vs. wild-type mice (A-D, n=3). The mRNA levels of the *MASP2* gene were normalized to *Gapdh* mRNA.

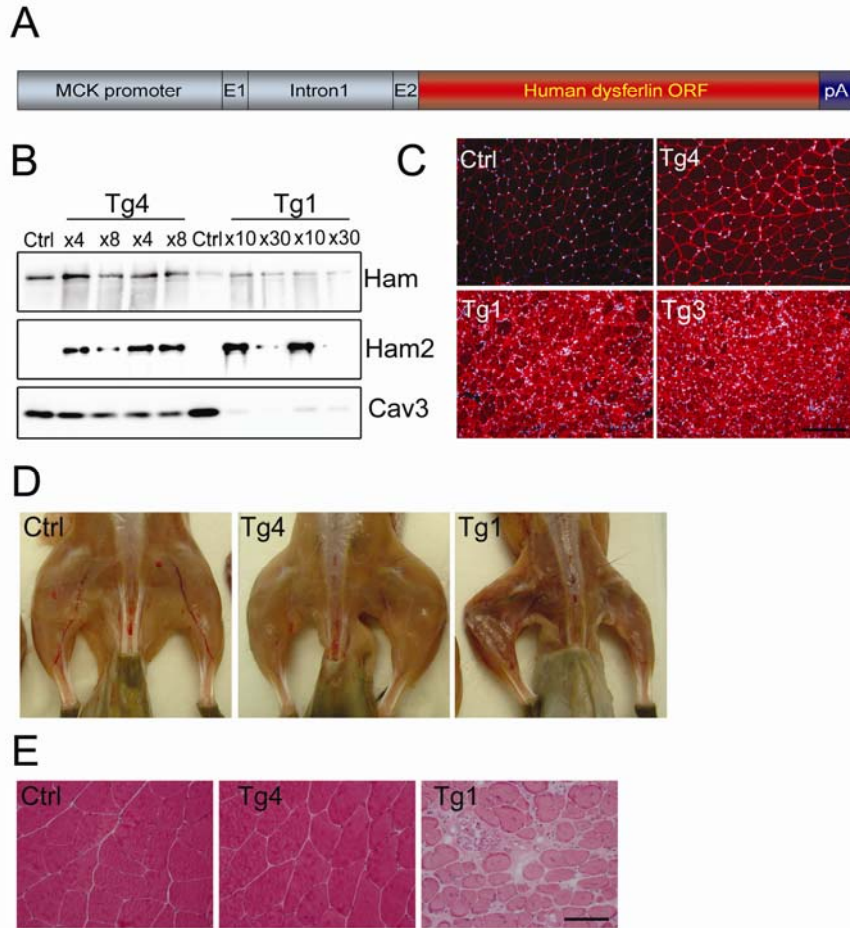


**Figure S2. Generation and characterization of muscle-specific dysferlin transgenic mice.** (A) Schematic diagram of the dysferlin transgene construct. To drive muscle-specific expression of dysferlin, the 6.5-kb mouse creatine kinase enhancer/promoter was fused to the human dysferlin cDNA followed by SV40 polyadenylation signal sequences. (B) Western blotting analysis of dysferlin expression in two transgenic lines (Tg4 and Tg1). Compared to the endogenous level in control littermates, dysferlin was overexpressed by ~8-fold and ~30-fold in Tg4 and Tg1, respectively. (C) Immunofluorescence staining analysis of muscle sections from the transgenic and control mice. Dysferlin immunofluorescence was increased in the sarcolemma and cytoplasmic punctate vesicles in the Tg4 line, while in the two high expression lines (Tg1 and Tg3), dysferlin was highly increased in the sarcolemma, cytosolic vesicles, but also accumulated in cytosolic aggregates. (D) Gross effect of dysferlin overexpression in muscle. High level of dysferlin overexpression in Tg1 resulted in severe muscle atrophy, while the low overexpression of dysferlin (Tg4) did not produce visible abnormality. (E) Representative H&E-stained histology of quadriceps muscles from WT, Tg4 and Tg1 mice. Scale bars: 200  $\mu$ m.

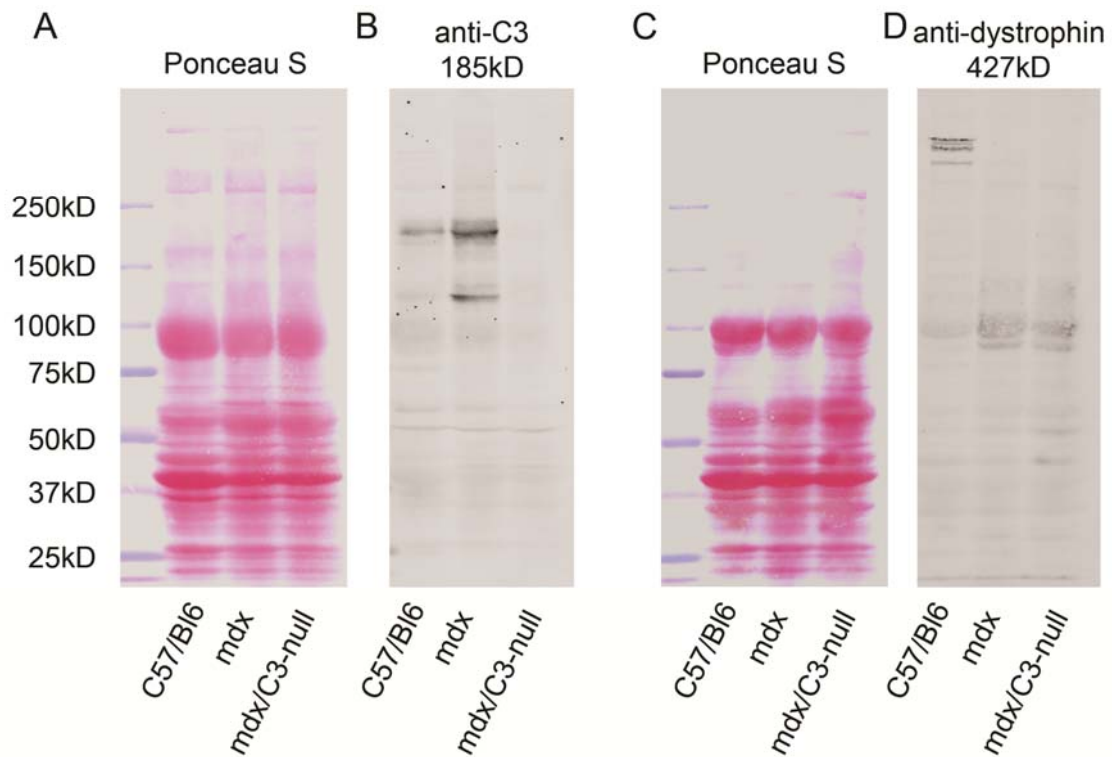


**Figure S3. Biochemical characterization of the *mdx/C3* mice.** The total muscle extracts of C57BL/6 (Lane 1), *mdx* (Lane 2) and *mdx/C3-null* (Lane 3) mice were blotted with the anti-C3 antibody (B) and the anti-dystrophin antibody (Mandra-1, D). The Ponceau S staining was performed to demonstrate the equal loading of samples in the different lanes. Note: The samples in C and D were reduced, but not in A and B.

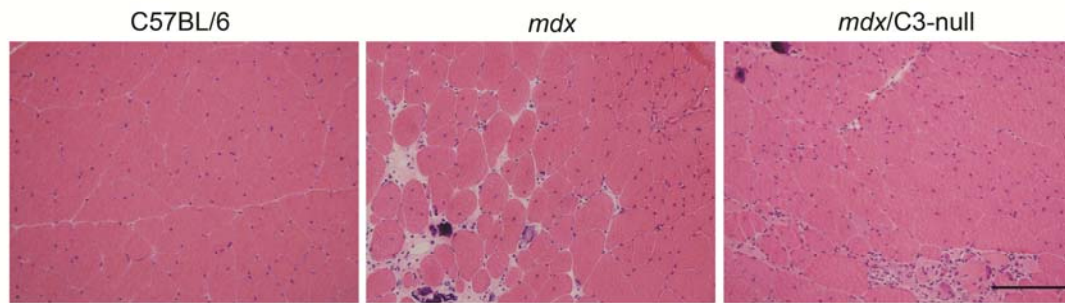


**Figure S4. Histological analysis of the *mdx/C3*-null mice.** H&E staining of the muscle cryosections from wild-type (WT), *mdx/C3*-null, and *mdx* mice showed that genetic ablation of C3 had not significantly improve the muscle pathology in *mdx* mice. Scale bar: 200  $\mu$ m.

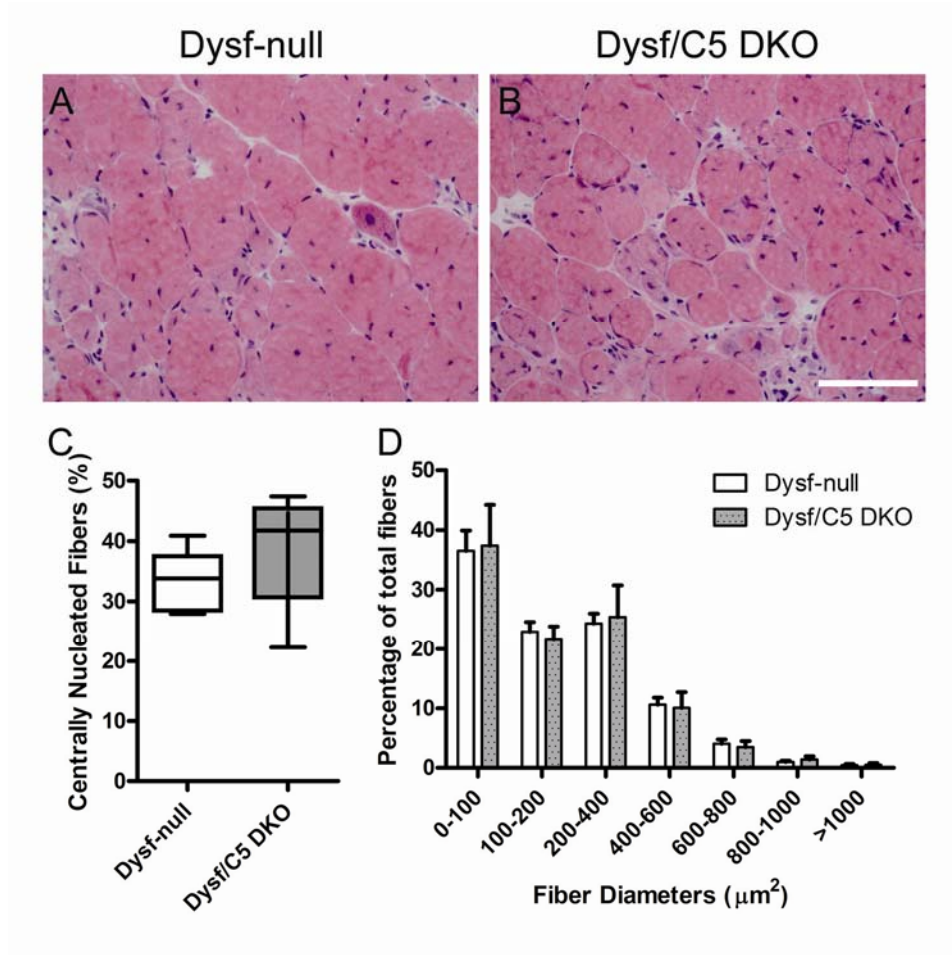


**Figure S5. Effect of genetic ablation of complement factor C5 on muscle pathology in dysferlin-deficient mice.** (A, B) Representative H&E-stained histology of quadriceps muscles from Dysf-null (A) and Dysf/C5 double-null littermate (B) at 23 weeks old. Scale bars: 100 μm. (C) Fiber areas (grouped into size ranges) from quadriceps muscles of 23-week-old Dysf/C5 double-null mice (N=5). (D) Percentage of fibers containing central nuclei in the quadriceps muscles of 23-week-old Dysf/C5 double-null mice (N=5). The Dysf-null data in C and D were re-plotted from **Figure 7 E** and **F**, respectively.

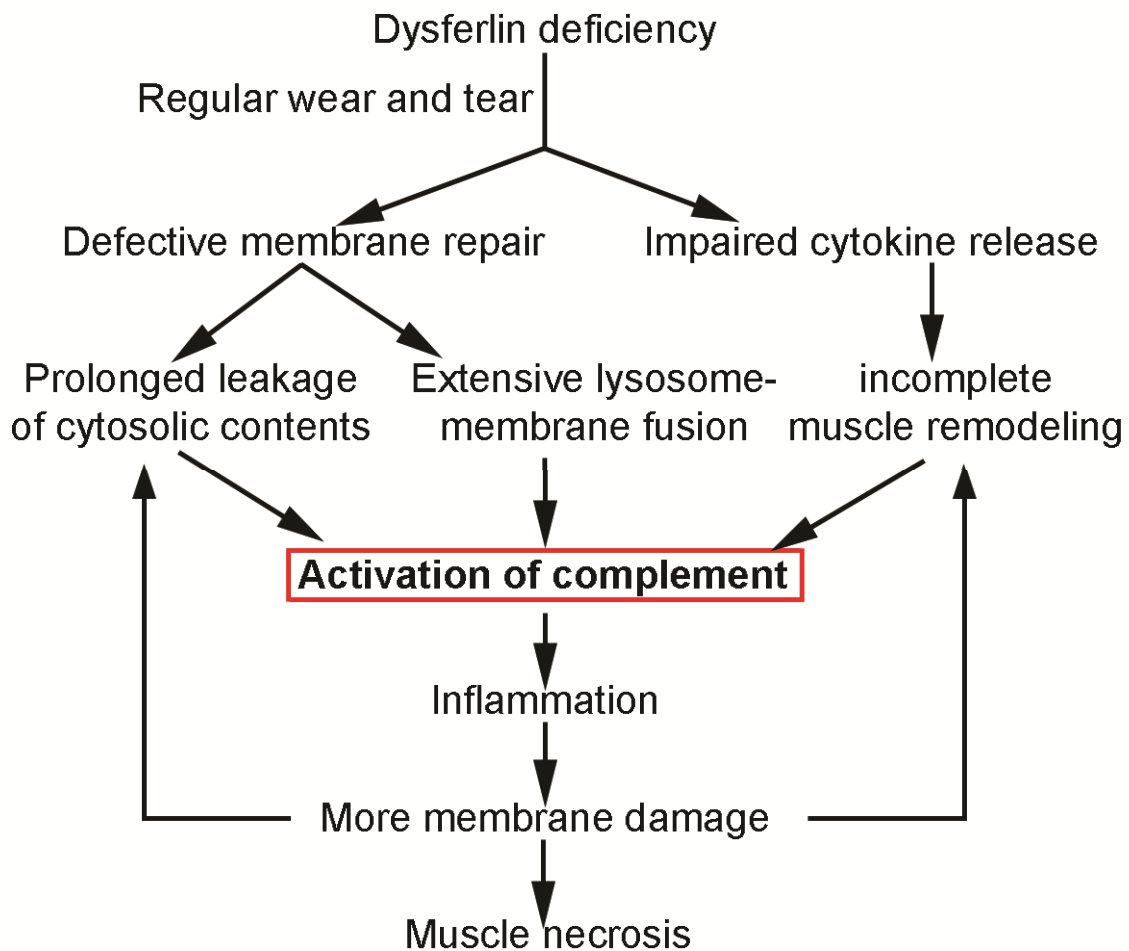


**Figure S6. Hypothetical mechanisms linking dysferlin deficiency with activation of the complement system in muscle.** Dysferlin deficiency causes defective membrane repair and impaired cytokine release. During regular muscle wear and tear, defective dysferlin-mediated membrane repair results in prolonged leakage of cytosolic contents and extensive lysosome-mediated membrane fusion may occur; while impaired cytokine release may account for delayed recruitment of neutrophils and incomplete muscle remodeling. These events could activate the complement system and cause muscle inflammation, resulting in more membrane damage and eventually leading to muscle necrosis.

## Supplemental Methods

**Mouse models.** Dysferlin-null mice (1) generated in our lab (backcrossed to C57BL/6J for six generations) and consomic dysferlin-null strain C57BL/6J-Chr 6A/J obtained from Jackson laboratory were used in this study. C3-null mice (B6.129S4-C3<sup>tm1Crj</sup>/J) generated in the laboratory of Dr. Michael C. Carroll (2) were obtained from Jackson laboratory and they were backcrossed to a C57BL/6J background for at least 6 generations. Consomic C5-null mice (C57BL/6J-Chr2<sup>A/J</sup>/NaJ) were purchased from Jackson Laboratory. Other mouse strains obtained from Jackson Laboratories include C57BL/6, *mdx*/C57BL/10ScSn (*mdx*), and SJL/J. The C5-null and C3-null were bred with dysferlin-null mice to generate dysferlin/C5 and dysferlin/C3 double mutant mice. The C3-null mice were bred with *mdx* mice to generate *mdx*/C3-null mice. Identification of mutant or transgenic mice was performed by PCR genotyping of genomic DNA prepared from mouse tail snips. Mice were maintained at the University of Iowa Animal Care Unit in accordance with the institute's animal usage guidelines. All animal studies were authorized by the Animal Care Use and Review Committee of The University of Iowa.

**Antibodies.** The mouse monoclonal antibodies Hamlet against dysferlin (Novacastra), Mandra-1 against dystrophin (Sigma-Aldrich), macrophage cell marker Mac-1 (University of Iowa Hybridoma Bank), T-lymphocyte marker CD3 (Sigma-Aldrich), B-lymphocyte CD20 (Sigma-Aldrich), caveolin-3 (Transduction Laboratories), C3 (MP Biochemicals), C5b-9 (Abcam, clone aE11), and polyclonal anti-laminin  $\alpha$  2-chain antibody (Alexis) were used for immunoblotting and immunofluorescence analysis. Alexa Fluor 488 or 555-conjugated secondary antibodies were obtained from Invitrogen.

**Generation of dysferlin transgenic mice.** The full-length human dysferlin cDNA was pieced together from a human cDNA library (a kind gift from Dr. Bento Soares), a clone DKFZp686K20163Q (RZPD, German) and a clone FLJ00175 (Kazusa DNA Research Institute, Japan) and the sequence was confirmed by the University of Iowa DNA Core Facility. The 6.3-kb human dysferlin cDNA was initially ligated into the KpnI site of the pEGFP-C3 vector to form pEGFP-hDysferlin. To drive muscle-specific expression of dysferlin, the 6.5 kb mouse myosin creatine kinase promoter (a kind gift from Jeff Chamberlain) ClaI (blunted)-XhoI fragment was ligated into AatI (blunted)-XhoI sites of pGem7zf followed by an SV40 polyadenylation signal which was PCR engineered with a 5' KpnI site and 3' NotI-SacI linker. The full-length human dysferlin was then cut from pEGFP-hDysferlin with KpnI and inserted into the KpnI site with correct orientation to generate the MCK-dysferlin construct in pGem7zf+. To produce the transgenic mice, the purified EcoRV-NotI 13-kb transgene fragment (Fig. 1) was microinjected into F1 hybrid zygotes from C57BL/6J X SJL/J parents by the University of Iowa Transgenic Animal Facility. The founders bearing a *Dysf<sup>im</sup>* allele were backcrossed with C57BL/6J mice two to three times. Since SJL mice contain a 171-bp deletion (*Dysf<sup>im</sup>*) in the dysferlin gene, the founder mice carry one *Dysf<sup>im</sup>* allele. Therefore, the F1 mice were also screened for *Dysf<sup>im</sup>* allele using forward and reverse primers 5'- TACAGCTGCTCTGTGGGTGG -3' and 5'- GTGCTGAGAATCAGGGTGGC-3', and any *Dysf<sup>im</sup>* allele carriers had been removed from the colony.

**Contractile properties.** Contractile properties were measured in vitro on extensor digitorum longus (EDL) muscles from C57BL/6 and dysferlin-null mice as described

previously(3). Mice were anesthetized by an intraperitoneal injection (I.P.) of 2% avertin (0.0015 ml/g body weight). Supplemental injections were administered to maintain an anesthesia level that prevented responses to tactile stimuli. Intact muscles were removed from each mouse after the mice were euthanized by an overdose of avertin, and the thoracic cavity was opened. Muscles were immersed in an oxygenated bath (95% O<sub>2</sub>, 5% CO<sub>2</sub>) that contained Ringer's solution (pH 7.4) at 25°C. For each muscle, one tendon was tied securely with a 5-0 suture to a force transducer (one end), and a servo motor (other end). Using twitches with pulse duration of 0.2 ms, the voltage or current of stimulation was increased to achieve a maximum twitch and then increased slightly. Twitches were then used to adjust the muscle length to the optimum length for force development (L<sub>0</sub>). The muscle length was set at L<sub>0</sub>, and EDL muscles were stimulated for 300 ms. Stimulation frequency was increased until the force reached a plateau at maximum isometric tetanic force (P<sub>0</sub>). The susceptibility to contraction-induced injury was measured during seven identical lengthening contractions each 400 ms long, with the contractions separated by a rest interval of 60 s. Muscles were activated maximally and following a delay of 100 ms, a lengthening ramp of 30% strain (or 40% for the group at 8 months of age) was initiated at a velocity of 1 Lf/s. The muscle was then returned L<sub>0</sub> at the same velocity. To assess the force deficit generated by this assay, a measurement of P<sub>0</sub> was made one minute after the last lengthening contraction. Based on measurements of muscle mass, muscle length, fiber length, and P<sub>0</sub>, the total fiber cross-sectional area and specific P<sub>0</sub> (kN/m<sup>2</sup>) were calculated. The data were analyzed by an analysis of variance (ANOVA). When the overall F-ratio for the ANOVA was significant, the differences between individual group means were determined by a single *t*-test. Significance was set *a priori* at P < 0.05. Data are expressed as mean ± SEM.

**Exercise-activity assay.** Mouse housing and exercise-activity rooms were under specific pathogen-free conditions. The exercise-activity assay was performed without anesthesia to avoid the impact of anesthesia on blood glucose and the blood flow to skeletal muscle. Locomotor activity was monitored by using Digiscan Animal Activity Monitoring System running Versamax Windows software (Accuscan Instruments). Mice were tested in individual chambers in sets of 4, for 30 x 1 minute intervals pre- and immediately post-exercise, at the same time every day in the dark, in an isolated room, and with the same handler. Data collected was converted to a Microsoft Excel worksheet and all calculations were done within the Excel program. Animals were mildly exercised using an adjustable variable speed belt treadmill from AccuPacer (AP4M-MGAG, AccuScan Instruments, Inc.), down a 15° grade at 15 mpm for 10 minutes with acclimatization at 3 mpm for 5 minutes.

### **Membrane repair assay**

The membrane repair assay was performed essentially as described (1, 3, 4). Briefly, isolated *flexor digitorum brevis* (FDB) muscle fibers were incubated in the Tyrode solution supplemented with 2.5  $\mu$ M FM 1-43 (Invitrogen). Membrane damage was induced in the presence of with a 2-photon confocal laser-scanning microscope (Zeiss LCS 510) coupled to a 10-W Argon/Ti:sapphire laser. After initial images were scanned, a 5- $\mu$ m  $\times$  5- $\mu$ m area of the sarcolemma of the muscle fiber was injury with 1.5-s irradiation at full power. Fluorescence images were captured at 10-second intervals for 5 min after the damage. The fluorescence intensities at the damaged site were quantified by using the ImageJ software (NIH) and plotted against the time after the damage.

**Serum Creatine Kinase Assays.** Blood for quantitative, kinetic determination of serum creatine kinase activity was collected either after the pre-exercise activity analysis or 2 hours post-exercise by mouse tail vein bleeds, using a Sarstedt microvette CB 300, from non-anesthetized restrained mice. Red cells were pelleted by centrifugation at 10,000 rpm for 4 minutes and serum was separated, collected and analyzed immediately without freezing. Serum creatine kinase assays were performed with an enzyme-coupled assay reagent kit (Stanbio Laboratory) according to manufacturer's instructions. Absorbance at 340 nm was measure every 30 sec for 2 min at 37°C so that changes in enzyme activity could be calculated.

**cDNA synthesis and real-time PCR assay.** Total RNA was isolated from skeletal muscle using TRIzol reagent (Invitrogen) and suspended in Dnase- Rnase-free distilled water (Invitrogen). First-strand complementary DNA (cDNA) was synthesized from total RNA using the AMV reverse transcriptase (Roche) and random hexamers, according to the manufacturer's instructions. Each of the target genes were real-time amplified from cDNA using oligonucleotides specific to each gene (sequences and conditions available upon request), and *Gapdh* or 28S-RNA was used as the normalization control. cDNA levels were determined using SYBR green in a MyiQ rt-PCR detection system (BioRad). All samples were run in triplicate.

**Immunofluorescence analysis.** Immunofluorescence staining for dysferlin, caveolin-3 (Cav3), Mac-1, CD3, C3, C5b-9, Lamp-2 was performed on 7 µm transverse muscle cryosections as described previously. For patient biopsies, immunofluorescence staining was

performed on serial cryosections. The anti-dysferlin antibody was purchased from Novocastra.

**Fiber area measurement.** Caveolin-3 or H&E stained cross sections of quadriceps at the middle belly from 10-week old dysferlin transgenic line 1, 4 and their control littermates were imaged with a Zeiss microscope at 40x magnification. The RGB images were then converted to 8-bit gray images and the fibre area was measured using Image Pro Plus 6 software.

### Supplemental References

1. Bansal, D., Miyake, K., Vogel, S.S., Groh, S., Chen, C.C., Williamson, R., McNeil, P.L., and Campbell, K.P. 2003. Defective membrane repair in dysferlin-deficient muscular dystrophy. *Nature* 423:168-172.
2. Wessels, M.R., Butko, P., Ma, M., Warren, H.B., Lage, A.L., and Carroll, M.C. 1995. Studies of group B streptococcal infection in mice deficient in complement component C3 or C4 demonstrate an essential role for complement in both innate and acquired immunity. *Proc Natl Acad Sci U S A* 92:11490-11494.
3. Han, R., Kanagawa, M., Yoshida-Moriguchi, T., Rader, E.P., Ng, R.A., Michele, D.E., Muirhead, D.E., Kunz, S., Moore, S.A., Iannaccone, S.T., et al. 2009. Basal lamina strengthens cell membrane integrity via the laminin G domain-binding motif of alpha-dystroglycan. *Proc Natl Acad Sci U S A* 106:12573-12579.
4. Han, R., Bansal, D., Miyake, K., Muniz, V.P., Weiss, R.M., McNeil, P.L., and Campbell, K.P. 2007. Dysferlin-mediated membrane repair protects the heart from stress-induced left ventricular injury. *J Clin Invest* 117:1805-1813.